J Solid State Eletrochem (2004) 8: 338–345
DOI 10.1007/s10008-003-0477-6

ORIGINAL PAPER

W. Plieth

Electrochemical deposition: the concept of residence times in structure development

Received: 9 July 2003 / Accepted: 4 November 2003 / Published online: 12 February 2004

Abstract The concept of the residence time of an atom in a kink position was introduced to predict the structure of electrochemically deposited surface coatings. The residence time is obtained from the reciprocal value of the rate constant for separation from the kink position. Residence times and deposition rates determine the density of kink positions [*ksp*] on the growing metal film. For equilibrium conditions (Nernst potential), the density of kink positions $[ksp]_0$ depends on the exchange current density i_0 and on the residence time τ by the equation:

$$[ksp]_0 = \frac{i_0 \tau N_L}{zF},$$

where N_L is Loschmidt's or Avogadro's number, F is Faraday's constant and z is the charge of the metal ions in the electrolyte. Calculated values of residence times are presented for pure metals as well as for silver–lead and nickel–aluminium alloys.

Keywords Kink positions · Nickel–aluminium alloy · Residence times · Silver–lead alloy · Surface coatings

Introduction

Electrochemical deposition of a thin metal, alloy or compound film is one of the oldest coating technologies. Electrochemical deposition offers unsurpassed advantages such as compactness or pore-free deposits, despite great advances made in plasma or vapour deposition technologies. With increasing demands for advanced coatings, the development of deposits with improved properties must be pursued. However, modifications must first be made as properties depend on the structure of the deposit and the structure depends on the deposition parameters, so that a better understanding of the influence of structure and of the structure forming processes on properties is necessary.

In the past, emphasis was put on depositing homogeneous metal or alloy phases, but, in recent years, new materials were developed by the formation of intermetallic compounds. Examples are superalloys with new high-temperature properties [1] or smart alloys showing the shape memory effect [2]. Even in the field of the classical corrosion protective zinc coating, the development of new alloys has definitely enhanced the performance. ZnNi alloys are one example. Up until now, the assumption was that the formation of an intermetallic phase, $Zn_{21}Ni_5$ (Zn with 14% Ni, γ-phase), was the reason for the corrosion protection of this composition [3], but recent experiments at lower Ni concentrations (deposition from alkaline electrolyte, 7–8% Ni) show that the δ-phase (Zn_8Ni) is formed. This phase segregates into pure Zn and the γ-phase after thermal treatment at 190 °C for 23 h [4]. The deposits from alkaline electrolytes show improved corrosion protection compared with the $Zn_{21}Ni_5$ deposits from acidic electrolytes.

Another example is zinc–manganese, where the formation of the δ_1-phase was observed at 10.7 wt% Mn [5]. In experiments on depositing alloys with a higher concentration of 20 wt% Mn, the X-ray diffraction pattern of the ϵ-phase was established [6]. It is also possible to deposit pure zinc with differing topographies (Fig. 1; Beyerhaus D, Plieth W, unpublished results), thus influencing the properties of this metal.

Structure determining factors

It is well known that the structure of an alloy is determined by the properties of its components. Hume-Rothery et al. [7] formulated rules for the formation of

Dedicated to the memory of Harry B. Mark, Jr. (28 February 1934–3 March 2003)

W. Plieth
Institute of Physical Chemistry and Electrochemistry, Technische Universitaet Dresden, 01062 Dresden, Germany
E-mail: waldfried.plieth@chemie.tu-dresden.de

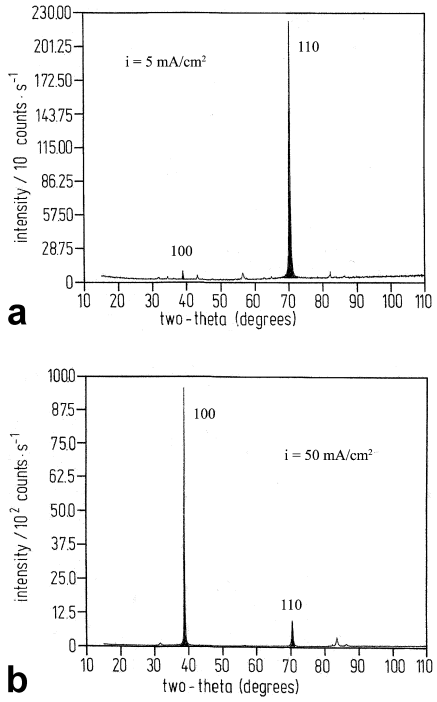

Fig. 1 X-ray diffraction peaks of Zn layers deposited from a commercial alkaline electrolyte with polyamine and other additives using different current densities: (**a**) 5 mA/cm^2; (**b**) 50 mA/cm^2 (Beyerhaus D, Plieth W, unpublished results)

solid solutions by comparing atomic diameters and electronegativities whereby both should not differ by more than 15%. The plotting of atomic radii and electronegativities versus group numbers shows that the position in the Periodic Table is a third important factor.

On inspecting the structure of copper–zinc alloys (brass), Hume-Rothery et al. [7, 8] observed that, at special values of the ratio of the number of valence electrons to the number of atoms in the Wigner–Seitz cell, transformations between different alloy phases occurred. Copper was crystallizing in the fcc lattice (Pearson symbol cF4). At a copper/zinc ratio of 1:1 (CuZn) and a valence electron/atom number ratio of 3:2 (21:14), the β-phase (W-type, Pearson symbol cI2) was formed. With a further increase of the zinc concentration at Cu_5Zn_8 (valence electron/atom number ratio of 21:13), the γ-phase (Cu_5Zn_8-type, Pearson symbol cI52) was observed. At $CuZn_3$ (valence electron/atom number ratio of 7:4 or 21:12), the ε-phase (Mg-type, hcp lattice, Pearson symbol hP2) was found.

Our modern knowledge and insight into the nature of the chemical bond tells us that electronegativity and valence electron concentration are aspects of the electrostatic and chemical interaction of the components, in principle enabling reduction of the factors responsible for the structure of a solid phase to three properties:

1. Size.
2. Coulomb forces by charge separation (ionic bonds).
3. Bond forces by localized or extended orbitals (covalent bonding or metallic bonding).

This, however, depends on the chemical nature of the components represented by the position in the Periodic Table. Therefore, in combination with the atomic number factor [9], these three factors lead to a successful classification and grouping of the elements. The results are structure tables, e.g. by Pettifor [10].

Bond energies

The various bonds in a solid (ionic, covalent, metallic) all contribute to the strength of the bond and to the solid-state properties; the bond strength is represented by the bond energy, which is one of the important parameters in characterizing a material. Even now, the determination of bond energies, especially for alloys, is not exactly a trivial task.

Bond energies of pure metals

In the case of the solid state of a pure metal, the bond energy can be calculated from the sublimation enthalpy $\Delta_S H$. This, the energy of an atom in the kink position, can be derived (Volmer [11] as discussed by Honigmann [12]; see also Budevski et al. [13], p 19):

$$\phi_{1/2} \approx \frac{\Delta_S H}{N_L} + \frac{1}{2}kT \qquad (1)$$

where N_L is the Loschmidt or Avogadro number. In the second term, k is the Boltzmann constant and T is the temperature; the second term is usually neglected ($< 1\%$). Volmer's approach is valid for evaporation of single atoms.

The value of $\phi_{1/2}$ is the characteristic value for the molecular interaction, and takes into account the interactions between first, second and further neighbours. For simple lattice models and pure metals it is exactly one half of the lattice energy of an atom. On application of an appropriate lattice model, it is possible to calculate the energy between two atoms. For example, in a close-packed hexagonal or cubic lattice with six close neighbours in the kink position, the results are approximately as follows:

$$\phi_{Me-Me} \approx \frac{\phi_{1/2}}{6} \qquad (2)$$

The second and third neighbours are not taken into consideration in this approach.

Bond energies of alloys

The situation for alloys is more complex, depending on the composition $A_{1-x}B_x$ and on the structure. To achieve approximate access to the interaction energy between atoms A and B, two procedures were suggested [14]. The first was based on the evaluation of the underpotential deposition (upd) potential of the

compact and fully discharged upd layer of the metal B on the substrate A. It was presumed that under these conditions the enthalpy difference for the formation reaction $Me_{bulk} \rightarrow Me_{upd}$ could be calculated.

The free energy (Gibbs energy) of formation of the upd modification of a metal is the following:

$$\Delta_f G_{upd} \approx -\frac{\Delta E_{upd}}{zF} \quad (3)$$

where ΔE_{upd} is the potential difference between the appropriate upd peak and the Nernst potential; z is the charge of the upd metal ions in solution, F the Faraday constant.

It was assumed that, for a compact and fully discharged upd layer, one could neglect the entropic term in $\Delta_f G_{upd}$ [14]. This assumption was based on the similar volume of vibration for an atom in the bulk and in the compact and fully discharged upd layer, as will be discussed in greater detail in a forthcoming publication [15]. Therefore it is possible to write the following:

$$\Delta_f G_{upd} \approx \Delta_f H_{upd} \quad (4)$$

Then one can calculate the sublimation enthalpy of the metal in its upd modification:

$$\Delta_S H_{upd} = \Delta_S H_{bulk} - \Delta_f H_{upd} \quad (5)$$

and hence the energy of an atom of the upd layer in a kink position of the upd layer, $\phi_{1/2,upd}$, by use of Eq. 1. From this value, the bond energy between atom A and atom B can be approximately derived using a crystallographic model of the upd layer on its substrate. An example of this process is the system Pb on Ag [16, 17].

In [14], a second possibility to derive approximate values of the bond energies between atoms A and B in an alloy is discussed. Using the potential dependence of the alloy composition in the region between the equilibrium potentials of A and B, but more positive than the equilibrium potential of B, the potential of commencing alloy formation E_f (Fig. 2) can be extrapolated. This potential is the analogue to the upd potential of B on A, in a similar way determined by the binding forces between A and B. It should be pointed out that the potential E_f is a potential near to the equilibrium potential and not at all far from the standard state of the metal, assuming that no kinetic effects determine the commencing alloy formation.

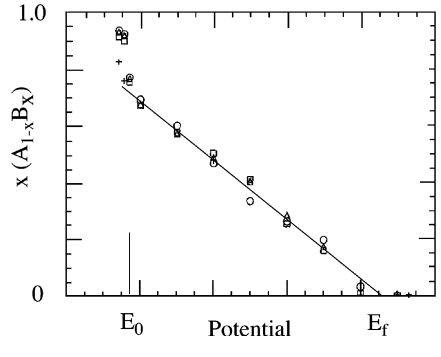

Fig. 2 Dependence of the alloy composition on the potential (schematic representation); extrapolation to the potential at the start of alloy formation, E_f; $\Delta E = E_f - E_0$ (E_0 is the equilibrium potential of the less noble component B) can be employed for bond energy calculations

The sublimation energy of the less noble alloy component B at zero concentration is obtained by a procedure similar to that described for upd layers. With the sublimation energy, the energy of B in a kink position of the alloy $A_{1-x}B_x$ for $x \rightarrow 0$ can be calculated with an equation similar to Eq. 1, which is the energy of an atom B in a pure matrix of atoms A. For the deposition of AlNi alloys, Moffat [18] recently measured several values. Bond energy values calculated by the procedures described for the examples mentioned are given in Table 2.

Theoretical calculation of bond energies

In the literature, attempts have been made to calculate bond energies theoretically, but a general solution to the problem is actually difficult. The problem lies in taking into account the differing contributions from Coulomb interactions, localized orbitals (covalent forces) and the contribution of delocalized orbitals (metal bonds). For an alloy AB, Miedema and co-workers [19] presented an empirical calculation of the formation ΔH_{AB}.

The concept of residence times in kink positions

Kink positions and rate equation of separation for a pure metal

In order to develop a mechanism leading from energy values to a prediction of the structure, the concept of the residence time of an atom in a kink position was introduced [20]; the kink position is the intermediate position of an atom in the crystallization process ([13], pp 16ff). Residence time (German word "Verweilzeiten"; in [20] the expression "dwell time" was used as it is more similar to the German expression "Verweilzeit", but the name "residence time" was recommended by one of the referees) is rarely used in electrochemistry. It describes the statistical time segment an atom stays in a kink position before separating again.

In the process of deposition, a metal ion on its way to discharging goes through three main intermediate states: the ad-atom position, the step position and the kink position [12, 13]. For each intermediate state the formation and separation reaction can be formulated. For each intermediate state, a residence time can be defined. In the following, exclusively the kink position will be discussed.

In Fig. 3 the kink position on a (100) face of a cubic primitive (cP) lattice is shown. Three various reaction paths exist for depositing and separating of a metal ion/

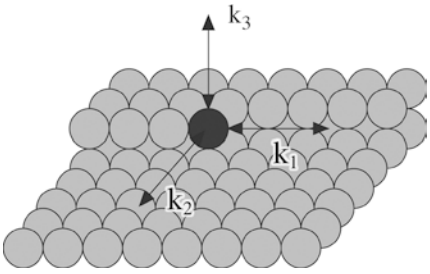

Fig. 3 Definition of the different reaction paths for separation from a kink position and deposition into a kink position; for simplicity, the cubic primitive (cP) lattice and a (100) face are depicted

metal atom to and from a kink position (the numbers differ from those in [20]: reaction path 3 in [20] is now reaction path 1 here, and vice versa):

1. Depositing from and separating to a step position. Figure 3 depicts a step running in the [100] direction.
2. Depositing from and separating to an ad-atom position.
3. Depositing from and separating into the ambient phase (gas phase or electrolyte; in the present paper the electrolytic phase is considered exclusively).

The three reactions for deposition and separation are parallel reactions. This is in contrast to the reactions in the mechanism of the deposition or dissolution process where these reactions are consecutive reactions.

For the definition of the residence time in the kink position, one only needs the separation reactions. The rate equation for the separation process is:

$$r_{\text{sep}} = k_{\text{sep}}[ksp] \tag{6}$$

where $[ksp]$ is the density of the kink positions an the surface. With three parallel separation reactions, the rate constant for separation, k_{sep}, consists of three terms:

$$k_{\text{sep}} = k_{\text{sep},1} + k_{\text{sep},2} + k_{\text{sep},3} \tag{7}$$

The various terms for the separation rate constant differ by the activation energy. Figure 3 depicts the (100) face of a primitive cubic lattice. In this example, and if solvation or complexing reactions are neglected, the activation energy required for separation from the kink position to a step position is almost equal to the breaking of one bond (approximately 1/3 of the energy of the kink position). The transfer to an ad-atom position is almost equal to the cleaving energy of two bonds (approximately 2/3 of the energy of the kink position) and the transfer to the ambient phase is almost equal to the cleaving energy of three bonds (approximately to the bond energy of the atom in the kink position).

With these values for the activation energy, the terms in the equation for the separation rate constant (Eq. 7) are given by the equations:

$$k_{\text{sep},1} = k_0 \exp\left(-\frac{\phi_{1/2}}{6kT}\right) \tag{8}$$

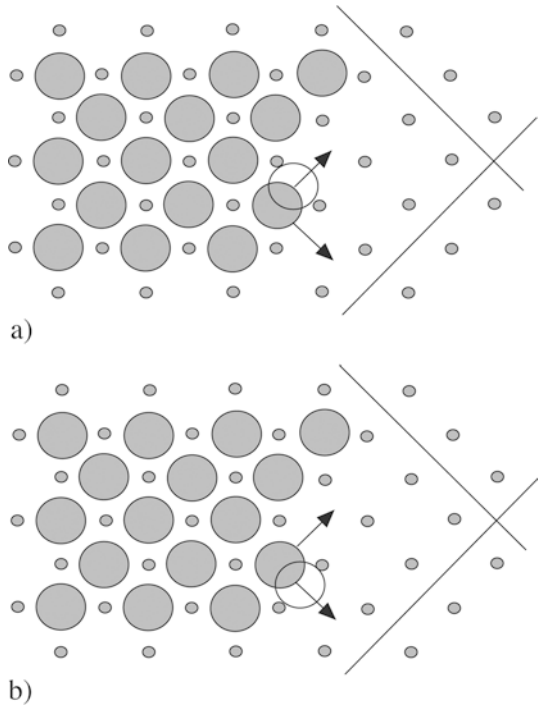

Fig. 4a, b Steps and kink positions of the (100) face of a cubic face-centred (cF, fcc) lattice; schematic representation. *Large spheres*: upper plane; *small spheres*: lower plane; the *lines* mark the main step directions on the (100) face. (**a**) Transition state to a step position; (**b**) transition state to an ad-atom position

$$k_{\text{sep},2} = k_0 \exp\left(-\frac{\phi_{1/2}}{3kT}\right) \tag{9}$$

$$k_{\text{sep},3} = k_0 \exp\left(-\frac{\phi_{1/2}}{kT}\right) \tag{10}$$

The constant k_0 is the rate constant for barrier-less separation (zero activation energy). The magnitude of k_0 is obtained from the frequency of dissociation; a typical value applied in transition state theory is 10^{12} s^{-1}.

In Fig. 4, the (100) face of a cubic face-centred (cF, fcc) lattice is shown. A variety of metals can crystallize in this structure. The transition state of the separation reactions in the surface plane are marked in Fig. 4 by open circles. The activation energies consist of two terms, one taking into account the cleavage of the bonds, another considering the activation energy of surface diffusion. The second term will be neglected, which is justified for electrified metal/electrolyte interfaces ([13], p 108). The influence of the solvation on the transition states is also neglected. Then the activation energy for the separation to a step position is:

$$E_{\text{a},1} = \phi_{\text{Me-Me}} = \phi_{1/2}/6 \tag{11}$$

and the activation energy for the separation to an ad-atom position is:

$$E_{\text{a},2} = 2\phi_{\text{Me-Me}} = \phi_{1/2}/3 \tag{12}$$

In this approach, an approximate value for the activation energy is used. It should be possible, in principle, to calculate the activation energy for appropriate models of the transition state.

With the suggested values for the activation energy, the terms in the equation for the rate constant of separation (Eq. 7) are given by the equations:

$$k_{\mathrm{sep},1} = k_0 \exp\left(-\frac{\phi_{1/2}}{6kT}\right) \tag{13}$$

$$k_{\mathrm{sep},2} = k_0 \exp\left(-\frac{2\phi_{1/2}}{6kT}\right) \tag{14}$$

$$k_{\mathrm{sep},3} = k_0 \exp\left(-\frac{\phi_{1/2}}{kT}\right) \tag{15}$$

Again, the constant k_0 is the rate constant for barrierless separation (zero activation energy) with an approximate value of 10^{12} s^{-1}.

A potential dependence (for electrochemical processes) can be introduced by a Butler–Volmer term P_i ($i = 1, 2, 3$) in Eqs. 8, 9, 10 and 13, 14, 15:

$$P_i = \exp\left(+\frac{\beta_i \Delta z_i e_0 U}{kT}\right) \tag{16}$$

and consists of a symmetry coefficient, β_i, describing the part of the electrode potential U (strictly speaking, the potential drop across the interface) influencing the different separation reactions, and the partial charge transfer, Δz_i, connected with the reaction steps 1, 2 and 3, respectively. The influence of the potential on the separation reactions in the surface plane is small. A stronger impact of the potential is expected for the direct separation to the electrolyte.

The energy of activation used in the previously mentioned equations is a relative value, enabling the kinetic comparison of the various paths of separation. With regard to the approximate nature of k_0, the present procedure is acceptable.

Kink positions and rate equations for the separation of an alloy

In order to transfer this concept to an alloy, it is necessary to define kink positions for alloys. In [20], this task was discussed for an AB alloy of equal stoichiometry (A:B = 1:1) and as well as crystallizing in a NaCl-type lattice (coordination number 6). Contrary to a pure metal, different kink positions have to be distinguished. For example, Fig. 5 depicts the (100) plane of an AB alloy with a NaCl-type lattice and for equal radii of the components.

Three nearest neighbours B surround an A atom in a "regular" kink position of this structure (kink site AB). In the next position, a deposited B atom is surrounded by three nearest neighbours A, again forming a regular kink position AB, whereby an A atom may also deposit

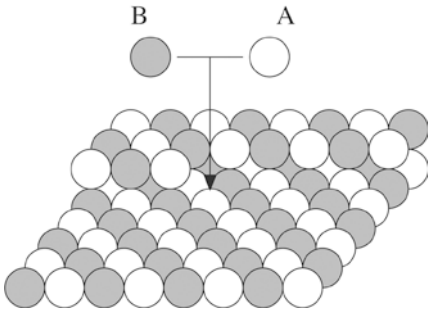

Fig. 5 Definition of kink positions on the 100 face of an alloy of composition AB, crystallizing in a NaCl-type lattice

in this position, then surrounded by three nearest A atoms, forming a kink position AA. If an atom B is deposited, the option for filling the following position is either an A atom in this position, again forming a regular kink position AB, or a B atom takes this position thus forming a kink position BB.

The separation reactions of a kink position AB can be described as follows:

1. The transfer to a step position, rate constant k_1: one bond AB must be cleaved and the activation energy is proportional to ϕ_{AB}.
2. The transfer to an ad-atom position, rate constant k_2: two bonds must be broken and the activation energy is proportional to $2\phi_{\mathrm{AB}}$.
3. Complete separation from the solid phase, transfer to the electrolyte or the gas phase, rate constant k_3: all bonds of the kink position must be cleaved and the activation energy is proportional to the full energy of the kink position.

As in the previous section, the general application approach could also be demonstrated at alloys crystallizing in the hexagonal or cubic close-packed structure. Kink sites on other planes and for other lattice types are described in [20].

The process of separation is described by rate equations similar to that applied for the pure metal (Eqs. 8, 9, 10 and 13, 14, 15) and knowing the bond energies between neighbouring atoms, ϕ_{AB}, ϕ_{AA} and ϕ_{BB}, the rate constants $k_{\mathrm{sep,AB}}$, $k_{\mathrm{sep,AA}}$ and $k_{\mathrm{sep,BB}}$ can be calculated approximately. The equation for the rate constant for separation from a kink position AB is given by:

$$k_{\mathrm{sep,AB}} = k_0 \left\{ \mathrm{e}^{-E_{\mathrm{a},1,\mathrm{AB}}/kT} + \mathrm{e}^{-E_{\mathrm{a},2,\mathrm{AB}}/kT} + \mathrm{e}^{-E_{\mathrm{a},3,\mathrm{AB}}/kT} \right\} \tag{17}$$

It consists of three terms, $E_{\mathrm{a},1}$, $E_{\mathrm{a},2}$ and $E_{\mathrm{a},3}$ for step transfer, ad-atom transfer and complete separation, respectively. The same equations exist for kink positions AA and BB. Under electrochemical conditions an additional factor P_i (Eq. 16) must be added to Eq. 17.

Using the values for ϕ_{AB}, ϕ_{AA} and ϕ_{BB} given in [14] and [15], approximate rate constants could be calculated. The results are shown in Table 2. In these calculations, solvation effects and the electrochemical factor were neglected.

Table 1 Pure metals of cubic close-packed structure (cubic face-centred lattice, Pearson symbol cF4). Enthalpies of melting, $\Delta_F H$, vaporization, $\Delta_V H$, and sublimation, $\Delta_S H$ [23]; energy of atoms in kink positions, $\phi_{1/2}$, rate constants of separation, k_{sep}, and residence times, τ

Metal	$\Delta_F H$(kJ/g-atom)	$\Delta_V H$(kJ/g-atom)	$\Delta_S H$(kJ/g-atom)	$\phi_{1/2}$ (eV)	$\phi_{1/2}/6$ (eV)	k_{sep} (s^{-1})	τ (s)
Al	10.7	293.7	304.4	3.15	0.526	1.3×10^{3}	7.6×10^{-4}
Pb	4.8	179.5	184.3	1.91	0.318	4.2×10^{6}	2.4×10^{-7}
Ni	17.8	380.6	398.4	4.13	0.688	2.4	4.2×10^{-1}
Rh	21.8	494.0	515.8	5.35	0.891	8.9×10^{-4}	1.1×10^{3}
Pt	21.7	447.0	468.7	4.86	0.810	2.1×10^{-2}	4.7×10
Cu	13.0	304.0	317.0	3.29	0.548	5.6×10^{2}	1.8×10^{-3}
Ag	11.3	254.0	265.3	2.75	0.458	1.8×10^{4}	5.5×10^{-5}
Au	12.8	324.4	337.2	3.49	0.582	1.5×10^{2}	6.9×10^{-3}

If the step mobility of the atoms A and B is restricted (as in the example of the [100] step direction in Fig. 5 for strong differences between ϕ_{AB}, ϕ_{AA} and ϕ_{BB}), the sequence of separation is modified in the sense that separation from the step substitutes the separation from the kink position.

The definition of residence times

The reciprocal value of the rate constant of separation is a time constant representing the mean time between the appearance of an atom in a kink position and its re-separation, thus named "residence time". The name "dwell time" was used in a previous publication ([20]).

The equation for residence time τ in a kink position of a pure metal is:

$$\tau = \frac{1}{k_{sep}} \tag{18}$$

It might appear that a definition like the half-life time (Eq. 18 multiplied by ln2) might be more appropriate, but for further use of τ the above definition is needed.

Examples for the residence times of pure metals with cubic close-packed structures (cubic face-centred lattices, Pearson symbol cF4), are given in Table 1.

The equations for residence times in the various kink positions of an AB alloy (as defined in Fig. 5) are:

$$\tau_{AB} = \frac{1}{k_{sep,AB}} \tag{19}$$

$$\tau_{AA} = \frac{1}{k_{sep,AA}} \tag{20}$$

$$\tau_{BB} = \frac{1}{k_{sep,BB}} \tag{21}$$

Table 2 Bond energies, $\phi_{Me\text{-}Me}$, rate constants of separation, k_{sep}, and residence times, τ. cF (fcc) lattice; (100) plane. The rate constants k_{sep} are calculated using the approximation $k_{sep} = k_{sep1}$

Alloy system	Bond	$\phi_{Me\text{-}Me}$ (eV)	k_{sep} (s^{-1})	τ (s)
Ag/Pb	Ag–Ag	0.458	1.7×10^{4}	6.1×10^{-5}
	Pb–Pb	0.318	4.0×10^{6}	2.5×10^{-7}
	Ag–Pb	0.418	7.9×10^{4}	1.3×10^{-5}
Al/Ni	Al–Al	0.526	1.2×10^{3}	8.7×10^{-4}
	Ni–Ni	0.688	2.0	4.9×10^{-1}
	Al–Ni	0.906	4.0×10^{-4}	2.5×10^{3}

Table 2 gives examples of the residence times for atoms in the kink positions AB, AA and BB for AgPb and AlNi. All components crystallize in the cubic close-packed structure [cubic face-centred (cF or fcc) lattice]. The intermetallic phase AlNi crystallizes in the CsCl structure, but is similar to the cubic close-packed structure.

The residence times are a transparent image of the stability of a kink position. In comparison to the deposition rates (next section), they provide the experimental conditions for predicting the formation of a special structure.

Rate of deposition, density of kink positions and structure of pure metals

The rate of deposition is measured by the deposition current, which calculates the number of atoms discharged per second and per unit of surface area. By multiplying this value together with the residence time, the number of atoms arriving during the residence time per unit of surface area, N_τ, is obtained:

Table 3 Density of kink positions at the Nernst potential $[ksp]_0$ calculated for some selected metals using the residence times of Table 1. Values of exchange current densities from [24]

Metal	Electrolyte	τ (s)	i_0 (A/cm^2)	$[ksp]_0$ (cm^2)
Ag	0.028 M $Ag(CN)_3^{2-}$; 1 M CN^-	5.7×10^{-5}	2.8×10^{-3}	1.0×10^{12}
	0.1 M $AgClO_4$; 1 M $HClO_4$	5.7×10^{-5}	4.5	1.6×10^{15}
	0.001 M $AgClO_4$; 1 M $HClO_4$	5.7×10^{-5}	1.5×10^{-1}	5.3×10^{13}
Cd	0.02 M $CdSO_4$; 1.6 M K_2SO_4	1.3×10^{-9}	1.5×10^{-3}	6.1×10^{6}
Cu	1.0 M $CuSO_4$; 1 M H_2SO_4	1.8×10^{-3}	1.0×10^{-10}	5.6×10^{5}
	0.1 M $CuSO_4$; 1 M H_2SO_4	1.8×10^{-3}	1.0×10^{-11}	5.6×10^{4}
Fe	1.0 M $FeSO_4$; 0.01 M H_2SO_4 (?)	7.0×10^{-2}	1.0×10^{-8}	2.2×10^{9}
Ni	0.5 M $NiSO_4$; pH 2.3 or 4.4	4.4×10^{-1}	1.0×10^{-6}	1.4×10^{12}
Zn	1.0 M $ZnSO_4$; 0.01 M H_2SO_4	3.8×10^{-9}	2.0×10^{-5}	2.4×10^{5}

$$N_\tau = \frac{i\tau N_L}{zF} \tag{22}$$

where N_L is Loschmidt's or Avogadro's number, F is Faraday's constant and z the charge of the metal ions in the electrolyte.

N_τ must be compared to the density of the kink positions, [*ksp*]. If N_τ is much smaller than [*ksp*], the number of kink positions will decrease; if N_τ is much larger than [*ksp*], the number of kink positions will increase. For stationary conditions ($t \to \infty$), the number of kink positions should approach the value of N_τ:

$$\lim_{t\to\infty} N_\tau = [ksp].$$

This leads to the following equation:

$$[ksp] \approx \frac{i\tau N_L}{zF} \tag{23}$$

A special state where stationary conditions can be expected is the electrochemical equilibrium potential (Nernst potential), when the density of kink positions $[ksp]_0$ is given by the exchange current density i_0 and the residence time:

$$[ksp]_0 = \frac{i_0\tau N_L}{zF} \tag{24}$$

For example, for an exchange current density of $i_0 = 10$ mA/cm^2, $z = 2$ and a residence time of $\tau = 10^{-3}$ s, the density of kink positions at the Nernst potential is 10^{13} cm^{-2}. Examples are given in Table 3.

The calculation of $[ksp]_0$ takes into account the nature of the metal (by τ) and the kinetic experimental conditions by i_0, reflecting the different experimental parameters such as electrolyte composition, additives, etc.

The density of kink positions under deposition conditions [*ksp*] is a factor determining the structure of the growing metal phase. At small current densities and small residence times, the crystal growth occurs at relatively few growths centres, producing the basic reproduction type (BR, in the notation of Fischer [21]). In other circumstances, high current densities and large residence times induce higher values of [*ksp*] and produce an irregular crystallographic structure: the field oriented texture type (FT), or the disoriented dispersion type (UD) is formed.

Some time ago, Winand [22] depicted a similar description in the form of an empirical diagram. In his diagram, the current density is plotted versus inhibitor concentration. Portraying a somewhat transparent explanation on a more quantitative basis, the current (x-axis) can be substituted by $i\tau$ while the inhibitor concentration (y-axis) can be substituted by $i_0\tau$.

Rate of deposition, density of kink positions and structure of alloys

Comparison of the residence time with the deposition rate is also possible for the deposition of an alloy. The deposition of an alloy of two components A and B of approximately similar size is chosen as an example. By a suitable selection of the experimental parameters (concentration of metal ions, complexing agents, potential, etc.), the deposition rate of A can be equalized to the deposition rate of B and be equivalent to equal partial current densities, $i_A \approx i_B$. Three such cases can be distinguished:

1. $\tau_{AB} \approx \tau_{AA} \approx \tau_{BB}$.

If a metal atom A or B is deposited in a kink position, then, independent of the character of the kink position, it will remain in this position (all kink positions are of equal stability). If during this time a second atom arrives (B or A), the position of the atom first deposited in the crystal lattice is established. The deposition rates are similar, but an attachment of atoms A or B is possible, leading to a homogeneous mixture between A and B and a solid solution.

It is possible to apply the concept of residence times, deposition rates and corresponding density of kink positions (as mentioned in the previous section) to this situation in the manner described. Deposition occurs with the rate $i = i_A + i_B$, and the residence times are approximately equal: $\tau_{AB} \approx \tau_{AA} \approx \tau_{BB} = \tau$. That means that Eq. 23 can be applied in order to calculate the expected density of kink positions, [*ksp*].

2. $\tau_{AB} << \tau_{AA} \approx \tau_{BB}$.

If the kink position AB is far less stable than the position AA or BB and at equal rates of deposition $i_A \approx i_B$, the formation of pure crystallites of atoms A and of atoms B is preferred. This situation is typical for the formation of a eutectic mixture. Under these conditions, individual kink positions of component A and component B on the surface are achieved. The equilibrium approach is given as follows:

$$[ksp]_A \approx \frac{i_A\tau_{AA}N_L}{zF} \tag{25}$$

$$[ksp]_B \approx \frac{i_B\tau_{BB}N_L}{zF} \tag{26}$$

3. $\tau_{AB} >> \tau_{AA}, \tau_{BB}$.

In this state the kink position AB is much more stable than AA or BB. If kink position AA or kink position BB is formed, it can be expected that either atom A or B separate from the kink position before the next attached atom stabilizes the position. If the kink position AB alone is formed, the atom in this position will dwell until the next built-in atom stabilizes its position. Under these conditions a crystallite AB (an intermetallic stable phase or intermetallic compound) is formed.

The number of kink positions characteristic of the stationary situation is given by:

$$[ksp]_{AB} \approx \frac{(i_A + i_B)\tau_{AB}N_L}{zF} \tag{27}$$

This must be compared with the values of $[ksp]_A$ and $[ksp]_B$ (Eqs. 25 and 26). When the deposition rate of one atom (e.g. A) grows considerably more than the other, the number of growth centres $[ksp]_A$ increases and matrix A develops, embedding the intermetallic phases AB. At very large deposition rates of A, this continues into a solid solution of few atoms B in the matrix of A.

Conclusions

The concept of residence times of atoms in kink positions was introduced in order to understand the electrochemical processes determining the development and growth of structures. The residence time is the reciprocal value of the rate of separation from the kink position. From the examples so far discussed, one obtains the impression that the residence time τ and deposition current density i (or exchange current density i_0 at the equilibrium potential) provide a measure of the surface dynamics and of the developing structure.

References

1. Anton DL (2000) In: Westbrook JH, Fleischer RL (eds) Structural applications of intermetallic compounds. Wiley, Chichester, p 1
2. Funakubo H (ed) (1987) Shape memory alloys. Gordon & Breach, New York
3. Bishop CV, Emch L, Block D, Freitas F (1998) Proc AESF-SUR/FIN, Ann Int Tech Conf, p 857; Chem Abstr CAN 130:299962
4. Gysen B (2003) Galvanotechnik 94:1090
5. Boshkov N (2003) Surf Coat Technol 172:217
6. Fels Ch (2002) Dissertation, Technische Universitaet Dresden
7. Hume-Rothery W, Smallman RE, Haworth CW (1969) The structure of metals and alloys, 5th edn. Institute of Metals, London, p 110
8. Mueller U (1992) Anorganische Strukturchemie, 2nd edn. Teubner, Stuttgart, pp 185–187
9. Villars P (2000) In: Westbrook JH, Fleischer RL (eds) Crystal structures of intermetallic compounds. Wiley, Chichester, pp 1–49
10. Pettifor DG (2000) In: Westbrook JH, Fleischer RL (eds) Crystal structures of intermetallic compounds. Wiley, Chichester, pp 195–214
11. Volmer M (1939) Kinetik der Phasenbildung. Steinkopf, Dresden
12. Honigmann B (1958) Gleichgewichts- und Wachstumsformen von Kristallen. Steinkopf, Darmstadt, p 93
13. Budevski E, Staikov G, Lorenz WJ (1996) Electrochemical phase formation and growth. VCH, Weinheim, p19
14. Plieth W (2003) Surf Coat Technol 169–170:96–99
15. Plieth W, Lorenz WJ, Staikov G (2004) J Solid State Electrochem (in press)
16. Bort H, Jüttner K, Lorenz WJ, Schmidt E (1978) J Electroanal Chem 90:41
17. Jüttner K, Lorenz WJ (1980) Z Phys Chem NF 122:163
18. Moffat P (1994) J Electrochem Soc 141:3059
19. de Boer FR, Boom R, Mattens WCM, Miedema AR, Niessen AK (1988) In: de Boer FR, Pettifor DG (eds) Cohesion in metals, transition metal alloys, vol 1, cohesion and structure. North-Holland, Amsterdam
20. Plieth W (2003) Z Phys Chem 217:383
21. Fischer H (1954) Elektrolytische Abscheidung von Metallen. Springer, Berlin Heidelberg New York
22. Winand M (1991) J Appl Electrochem 21:377
23. D'Ans-Lax (1967) Taschenbuch fuer Chemiker und Physiker, 3rd edn, vol 1. Springer, Berlin Heidelberg New York, p 81
24. Vetter KJ (1961) Elektrochemische Kinetik. Springer, Berlin Heidelberg New York, p 525